Inhibition of Human Steroid 5α Reductases type I and II by 6-Aza-Steroids: Structural Determinants of One-Step vs Two-Step Mechanism

Marcia L. Moss,*,‡ Petr Kuzmič,§ J. Darren Stuart,‖ Gaochao Tian,‡ Anne G. Peranteau,‡ Stephen V. Frye,⊥
Sue H. Kadwell,# Thomas A. Kost,# Laurie K. Overton,# and Indravadan R. Patel#

*Departments of Enzymology, Receptor Biochemistry, Protein Chemistry, and Medicinal Chemistry, Glaxo Wellcome,
5 Moore Drive, Research Triangle Park, North Carolina 27709, and School of Pharmacy, University of Wisconsin,
425 North Charter Street, Madison, Wisconsin 53706*

Received October 17, 1995; Revised Manuscript Received January 17, 1996⊗

ABSTRACT: We have discovered that 17β-[*N,N*-(diethyl)carbamoyl]-6-azaandrost-4-en-3-one is a time-dependent inhibitor of type II 5α-reductase, as is the drug finasteride. Unlike finasteride, the 6-aza-steroid is not a time-dependent inhibitor of type I 5α-reductase. Finasteride inhibition of type II enzyme proceeds in a two-step mechanism. At pH 6 and 37 °C, an initial finasteride−reductase complex is formed with a K_i^{app} of 11.9 ± 4.1 nM. In a second step, an irreversible complex is formed with a rate constant of inactivation of 0.09 ± 0.01 s^{-1}. In contrast, the 6-aza-steroid is a reversible inhibitor. From the results of a simplified mathematical analysis, based on the rapid equilibrium approximation, the inhibitor and the enzyme form an initial complex with a K_i of 6.8 ± 0.2 nM. The reversible formation of a final complex, with an overall K_i of 0.07 ± 0.02 nM, is characterized by a first-order isomerization rate constant 0.0035 ± 0.0001 s^{-1} for the forward step and 0.00025 ± 0.00006 s^{-1} for the backward step. All rate constants for the two-step mechanism were obtained by using a general numerical integration method. The best fit values for the association and dissociation rate constants were 5.0 μM^{-1} s^{-1} and 0.033 ± 0.008 s^{-1}, respectively, and the isomerization rate constants were 0.0035 ± 0.0007 s^{-1} and 0.000076 ± 0.000019 s^{-1}. These values correspond to an initial K_i of 6.5 nM and an overall dissociation constant of 0.14 nM. The data presented here show that both finasteride and the 6-aza-steroid analogs are potent against type II 5α-reductase, although their mechanisms of inhibition are different.

Dihydrotestosterone (DHT)[1] plays a key role in the maintenance of the mammalian prostate. The androgen has been associated with benign prostatic hyperplasia (BPH), a disease that is prevalent in elderly males (Wilson, 1980). Early symptoms of BPH include obstructive urinary voiding and nocturia. However, a prostatectomy is often required when progression of the disease causes repeated infection, bleeding, or hydronephrosis (Smith et al., 1988). A therapeutic approach to alleviating symptoms of BPH may be by lowering DHT levels via inhibition of steroid 5α-reductases (5-AR).

Steroid 5α-reductases are membrane-bound enzymes that catalyze the NADPH-dependent reduction of testosterone to dihydrotestosterone. Two types of 5α-reductase have been identified (Anderson & Russell, 1990; Anderson et al., 1991).

In humans, the type I enzyme predominates in the sebaceous glands of skin and the liver, while type II 5-AR is most abundant in the prostate, seminal vesicles, liver, and epididymis (Thigpen et al., 1993). Inhibitors of the reductases have been described, and one of these compounds, 17β-[*N*-(1,1-dimethylethyl)carbamoyl]-4-azaandrost-1-en-3-one, or finasteride (Figure 1), is currently approved for use in the treatment of BPH. Previous reports have described finasteride to be a competitive, reversible inhibitor of human type I and II 5α-reductases with inhibition constants of 300 and 10 nM, respectively (Liang et al., 1985; Anderson et al., 1991; Jenkins et al., 1992). More recently, finasteride was reported to be a slow binding inhibitor of the type I (Tian et al., 1994) and type II enzymes (Faller et al., 1993). As a result of the slow binding, the inhibitory potency of the drug had been underestimated.

In the case of type I reductase, finasteride forms an initial reversible complex EI with an inhibition constant of 360 nM at pH 7 and 37 °C. Effectively irreversible inhibition occurs in a subsequent slow step with a rate constant of 0.0014 s^{-1} to generate a final enzyme−inhibitor complex EI* (Tian et al., 1994). The half-life for the recovery of activity from EI* is greater than 3 days. In contrast, with type II reductase the dissociation constant of the initial complex has not been determined, and the overall inhibition constant was estimated to be less than 1 nM. Recovery of activity, however, was not observed after overnight dialysis of the complex (Faller et al., 1993). In this paper we investigated the time-dependent inhibition of type II enzyme in detail and determined the kinetic constants for the irreversible two-step mechanism.

---

* Address correspondence to this author at Glaxo Wellcome, 5 Moore Dr., Research Triangle Park, NC 27709. Telephone: (919) 483-6695. Fax: (919) 941-4320.
‡ Department of Enzymology, Glaxo Wellcome.
§ University of Wisconson.
‖ Department of Receptor Biochemistry, Glaxo Wellcome.
Department of Protein Chemistry, Glaxo Wellcome.
⊥ Department of Medicinal Chemistry, Glaxo Wellcome.
⊗ Abstract published in *Advance ACS Abstracts,* March 1, 1996.
[1] Abbreviations: finasteride **1**, 17β-[N-(1,1-dimethylethyl)carbamoyl]-4-azaandrost-1-en-3-one; **2**, 17β-[*N,N*-diethylcarbamoyl]-4-azaandrostan-3-one; **3**, 17β-[*N,N*-diethylcarbamoyl]-6-azaandrost-4-en-3-one; **4**, 17β-[*N,N*-diethylcarbamoyl]-4-methyl-6-azaandrost-4-en-3-one; **5**, 17β-[*N,N*-diethylcarbamoyl]-6-methyl-6-azaandrost-4-en-3-one; **6**, 17β-[*N,N*-diethylcarbamoyl]-6-acetyl-6-azaandrost-4-en-3-one; HPLC, high-performance liquid chromatography; K_i, inhibition constant; DMSO, dimethyl sulfoxide; DHT, dihydrotestosterone; 5-AR, 5α-reductase; BPH, benign prostatic hyperplasia.
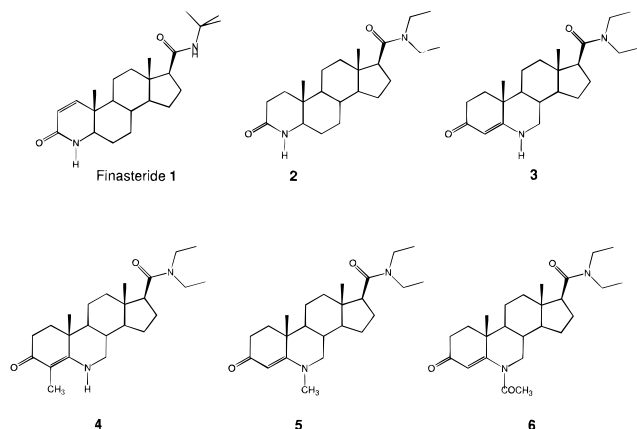
FIGURE 1: Structures of the 4-aza-steroids, finasteride **1**, 17-*N*,*N*-diethylcarbamoyl-4-aza-5-androstan-3-one **2**, and the 6-aza-steroids, 17β-[*N*,*N*-(diethyl)carbamoyl]-6-azaandrost-4-en-3-one **3**, 17β-[*N*,*N*-(diethyl)carbamoyl]-4-methyl-6-azaandrost-4-en-3-one **4**, 17β-[*N*,*N*-(diethyl)carbamoyl]-6-aza-*N*-methyl-androst-4-en-3-one **5**, and 17β-[*N*,*N*-(diethyl)carbamoyl]-6-aza-*N*-acetyl-androst-4-en-3-one **6**.

We have recently described 6-aza-steroids as potent dual inhibitors of type I and II 5-AR (Frye et al., 1993, 1994). In this paper we show that several 6-aza-steroids are not only potent but also time-dependent inhibitors of type II enzyme. We characterize the mechanism of inhibition of a member of a novel class of 6-aza-steroids, the inhibitor 17β-[*N*,*N*-(diethyl)carbamoyl]-6-azaandrost-4-en-3-one, and compare its kinetic properties with finasteride.

EXPERIMENTAL PROCEDURES

Materials. [1,2,6,7-³H(N)]Testosterone was purchased from DuPont NEN Research Products. Testosterone, NAP-DH, DTT, glucose 6-phosphate, and glucose 6-phosphate dehydrogenase were products of Sigma. Finasteride (**1**) was obtained from Lancaster Synthesis Ltd. 17β-[*N*,*N*-Diethyl-carbamoyl]-4-azaandrostan-3-one (**2**) was synthesized by known methods (Rasmusson et al., 1986). 17β-[*N*,*N*-Diethylcarbamoyl]-6-azaandrost-4-en-3-one (**3**), 17β-[*N*,*N*-diethylcarbamoyl]-4-methyl-6-azaandrost-4-en-3-one (**4**), 17β-[*N*,*N*-diethylcarbamoyl]-6-methyl-6-azaandrost-4-en-3-one (**5**), and 17β-[*N*,*N*-diethylcarbamoyl]-6-acetyl-6-azaandrost-4-en-3-one (**6**) were synthesized according to Frye et al. (1993).

Plasmid Construction. The plasmid 5α-reductase II-pBS containing a cDNA of the human type II 5α-reductase was kindly provided by Dr. David Russell. Synthetic oligonucleotides and site-directed mutagenesis were used to create *Nhe*I restriction sites immediately 5′ and 3′ of the coding sequence of the cDNA (GCTAGCATG–5α-reductase 2 coding sequence–TAA GCTAGC). The coding sequence was then subcloned into the *Nhe*I site of the baculovirus transfer plasmid pJVP10Z (Vialard et al., 1990). In this plasmid the 5α-reductase 2 gene is placed downstream of the viral polyhedrin promoter, and the bacterial gene coding for the enzyme α-galactosidase is cloned downstream of the viral p10 promoter. This plasmid is designated hu 5α-reductase 2-pJVP10Z. Types I and II 5α-reductase were prepared from SF-9 cells as described previously (Tian et al., 1994).

Demonstration of the Time Dependence of Inhibition. For the type I reductase, the inhibitor (0.5–1 μM) was added from a 1 mM stock solution in DMSO to 15 nM enzyme in 2.25 mL of standard buffer containing 17.6 mM imidazole, 17.6 mM diethanolamine, 0.3 M KCl, 13.2 mM succinic acid,

1 mM DTT at pH 7.0 or 6.0 and 37 °C, 1.0 mM NADPH, and a regenerating system consisting of 1 mM glucose 6-phosphate and 12 units/mL glucose 6-phosphate dehydrogenase. After 0–30 min of preincubation, 50 μL of the enzyme–inhibitor mixture was added into 150 μL of a 1 μM solution of [³H]testosterone in the standard buffer at 37 °C. After 1 min, the reaction mixture was quenched with 100 μL of absolute ethanol. The conversion of tritiated testosterone to dihydrotestosterone was quantified as described previously (Tian et al., 1994). The residual enzyme activity was expressed as the amount of product formed per unit of time, assuming constant reaction rate over the assay time. For the type II enzyme, the inhibitor at a concentration of 10 nM was added to 4 nM enzyme. The mixture was incubated under the same conditions as above, in a final volume of 1.5 mL. The amount of product formed was measured after first adding 100 μL of the enzyme–inhibitor mixture.

Initial Apparent Inhibition Constants. Stock solutions of inhibitors were prepared in DMSO. Inhibition studies were performed by adding 50 μL of type II enzyme, 0.2–0.4 nM, to 50 μL of a solution of 5 nM [1,2,6,7-³H(N)]testosterone in standard buffer containing varying concentrations of inhibitor. Reactions were quenched after 1 min by the addition of 100 μL of absolute ethanol. Conversion of testosterone to dihydrotestosterone was quantified by radiochemical analysis of peaks separated by HPLC. Relative enzymatic activity, R, was computed from the ratio of product amounts obtained in the presence and absence of inhibitors as $R = 1 - [P]/[P]_0$. The relative inhibition was fit by nonlinear least-squares regression to eq 1, where $[I]_0$ is the total concentration of inhibitor and K_i^{app}, the fitting parameter, is the apparent inhibition constant.

$$R = [I]_0/(K_i^{app} + [I]_0) \tag{1}$$

Time Dependence of Apparent Inhibition Constants. Experiments were conducted as described above, except that the type II enzyme was added to inhibitors at varying concentrations, and then assayed after preincubation for 0, 10, or 20 min.

Recovery of Activity from Inactivated Type II 5α-Reductase. The type II enzyme, 10 nM, was inactivated by addition of 20 nM inhibitor in a final volume of 150 μL. After a 30 min incubation at 37 °C, the microsomes were pelleted by centrifugation at 70K in a 100.3 rotor and Beckman Table top ultracentrifuge. The supernatant was removed, and the pellet was resuspended in 1.3 mL of standard buffer containing 1 μM tritiated testosterone. At time intervals from 0 to 60 min, the percent conversion of testosterone to dihydrotestosterone was followed by injection of an aliquot onto a reversed phase C18 column as described previously (Tian et al., 1994).

Measurement of the Reaction Progress. Several Eppendorf tubes were prepared containing 0.3–24 nM finasteride and 16 nM [1,2,6,7-³H(N)]testosterone in 1.04 mL of standard buffer. To each tube, 60 μL of enzyme, 50–100 pM, was added to initiate the reaction. Aliquots were removed from 10 s to 10 min and quenched with excess ethanol. Product formation was monitored as described above. For experiments with **3**, inhibitor concentrations varied from 8 to 68 nM and the testosterone concentration was 31 nM.

Substrate Progress Curve Analysis. The percentage of product formed, p, vs reaction time, t, was fitted to the recursive integral rate eq 2, a variant of a known method

$$p^{(m+1)} = p^{(m)} + r_{\mathrm{P}}(1 - [\mathrm{P}]/[\mathrm{S}]_0 - \exp\alpha)/(1/[\mathrm{S}]_0 - \exp\alpha/K_{\mathrm{M}}) \quad (2)$$

$$\alpha = ([\mathrm{P}] - tV_{\mathrm{max}})/K_{\mathrm{M}} \quad (2a)$$

$$[\mathrm{P}] = (p^{(m)} - p_0)/r_{\mathrm{P}} \quad (2b)$$

for the estimation of K_{M} and V_{max} from the reaction progress (Duggleby, 1986). The instrumental offset parameter p_0 accounts for the possible systematic error of the detection method. Other optimized parameters in the least-squares regression were the specific molar instrumental response of the reaction product r_{P}, the Michaelis constant K_{M}, and the maximum velocity V_{max}. The fixed parameter were the mixing delay time ($t_{\mathrm{D}} = 0$) and the initial substrate concentration $[\mathrm{S}]_0$. Auxiliary variables α and $[\mathrm{P}]$ are defined in equations (2a) and (2b).

Inhibitor Progress Curve Analysis. The reaction time course in the presence of finasteride or inhibitor **3** was fitted to eq 3, which is a modification of the standard burst kinetic

$$p = p_0 + v_{\mathrm{s}}t + (v_{\mathrm{o}} - v_{\mathrm{s}})[1 - \exp(-k_{\mathrm{app}}t)]/k_{\mathrm{app}} \quad (3)$$

model (Morrison & Walsh, 1988; Morrison, 1982). In this version, the instrumental offset p_0 is treated as an adjustable parameter, to account for the possibility of systematic errors in measuring the product conversion degree (HPLC with radiometric detection). Each individual progress curve was fitted separately. The local fitting parameters were the initial velocity v_0, the steady-state velocity v_{s}, the apparent first-order rate constant k_{app}, and the instrumental offset p_0. These fitting parameters were analyzed to extract approximate inhibition constants, as is described in the Discussion.

In the case of inhibitor **3**, a more general method of analysis was used also. Several reaction progress curves, obtained in the presence and absence of inhibitor **3** at various concentrations, were combined and fitted as a whole. The fitting model was the eq 4, in which the concentration of

$$p = p_0 + r_{\mathrm{p}}[\mathrm{P}]_t \quad (4)$$

product $[\mathrm{P}]_t$ at time t is obtained by numerical integration of the system of differential eqs 5a−g.

$$d[\mathrm{E}]/dt = -k_1[\mathrm{E}][\mathrm{S}] + (k_2 + k_3)[\mathrm{ES}] - k_4[\mathrm{E}][\mathrm{I}] + k_5[\mathrm{EI}] \quad (5a)$$

$$d[\mathrm{S}]/dt = -k_1[\mathrm{E}][\mathrm{S}] + k_2[\mathrm{ES}] \quad (5b)$$

$$d[\mathrm{ES}]/dt = k_1[\mathrm{E}][\mathrm{S}] - (k_2 + k_3)[\mathrm{ES}] \quad (5c)$$

$$d[\mathrm{P}]/dt = k_3[\mathrm{ES}] \quad (5d)$$

$$d[\mathrm{I}]/dt = -k_4[\mathrm{E}][\mathrm{I}] + k_5[\mathrm{EI}] \quad (5e)$$

$$d[\mathrm{EI}]/dt = k_4[\mathrm{E}][\mathrm{I}] - (k_5 + k_6)[\mathrm{EI}] + k_7[\mathrm{EJ}] \quad (5f)$$

$$d[\mathrm{EJ}]/dt = k_6[\mathrm{EI}] - k_7[\mathrm{EJ}] \quad (5g)$$

Numerical integration of the differential system (eqs 5a−g) was performed by using the Livermore Solver of Ordinary Differential Equations (LSODE, Hindmarsh, 1983). A modification of the Marquardt−Levenberg least-squares fitting algorithm (Reich, 1992) was used to perform the regression of experimental data. The optimized fitting parameters were all rate constants except the bimolecular association rate constant k_1, the total enzyme concentration $[\mathrm{E}]_0$ for each progress curve (within 10% titration error), the molar response coefficient r_{P}, and the offset p_0 for each progress curve. The regression analysis was performed by using the computer program DYNAFIT (BioKin, Ltd., Madison, WI).

RESULTS

Substrate Kinetics. Knowledge of the substrate kinetic parameter was a prerequisite for analyzing properly the inhibition data. A preliminary analysis was performed by using the standard initial velocity method, which gave K_{M} of 7 μM for the type I reductase, and K_{M} of approximately 10 nM for the type II enzyme under the conditions used in the inhibition assays. A more accurate estimate of K_{M} and V_{max} for type II reductase came from the analysis of the substrate progress curve. Figure 2 shows the results of nonlinear least-squares fit to eq 2. The initial substrate concentration, $[\mathrm{S}]_0$, was fixed at 31 nM, while the best-fit values of the adjustable fitting parameters were $V_{\mathrm{max}} = 0.031 \pm 0.002$ nM s^{-1}, $K_{\mathrm{M}} = 20.5 \pm 3.0$ nM , $r_{\mathrm{P}} = 3.21 \pm 0.04$ au nM^{-1}, and $p_0 = -1.03 \pm 0.54$ au. The arbitrary unit (au) of molar response is defined as percent of product formed in the reaction. From the results of fit, the maximum velocity expressed in the arbitrary units is $3.21 \times 0.031 = 0.098\%$ of product per second, and, for control, the maximum conversion is $3.21 \times 31 + 1.03 = 100.5\%$ of product.

To investigate the possibility of product inhibition, progress curves were collected at different substrate concentrations (8, 16, 40, 80, and 160 nM, data not shown). The data were fitted simultaneously to the mathematical model for the simple Michaelis−Menten reaction mechanism, represented by the system of differential equations (eqs 6a−d) and the

$$d[\mathrm{E}]/dt = -k_1[\mathrm{E}][\mathrm{S}] + (k_2 + k_3)[\mathrm{ES}] \quad (6a)$$

$$d[\mathrm{S}]/dt = -k_1[\mathrm{E}][\mathrm{S}] + k_2[\mathrm{ES}] \quad (6b)$$

$$d[\mathrm{ES}]/dt = k_1[\mathrm{E}][\mathrm{S}] - (k_2 + k_3)[\mathrm{ES}] \quad (6c)$$

$$d[\mathrm{P}]/dt = k_3[\mathrm{ES}] \quad (6d)$$

response function (eq 4).

While the bimolecular association rate constant k_1 was kept constant at 10^8 M^{-1} s^{-1}, as was the assumed enzyme concentration (0.01 nM), the best-fit values of the remaining rate constants were $k_2 = 1.48 \pm 0.57$ s^{-1} and $k_3 = 0.644 \pm 0.024$ s^{-1}; the calculated substrate dissociation constant is thus 14.8 ± 5.7 nM. The important finding is that all progress curves taken together fit very well to the simple
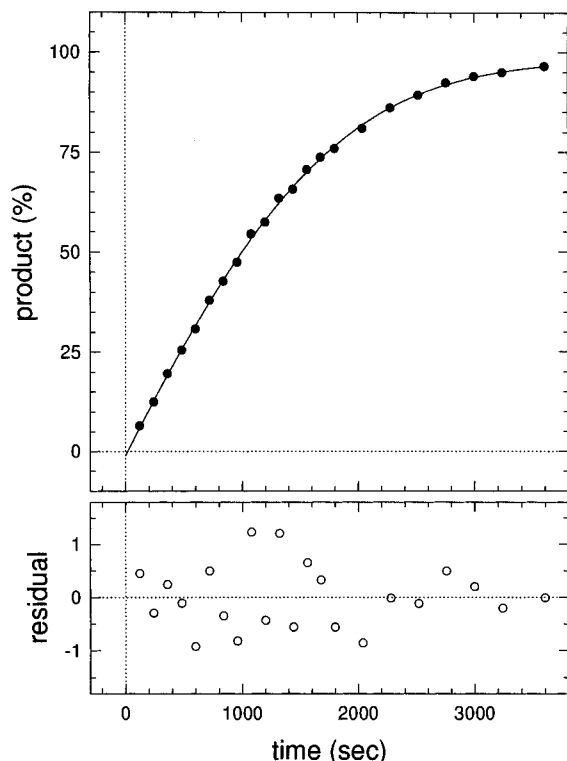
FIGURE 2: Least-squares fit of substrate progress curve (0.05 nM 5α-reductase II, 31 nM testosterone, pH 6.0, 37 °C) to the modified integral Michaelis–Menten eq 2. The best-fit values and standard errors of adjustable parameters were $V_{max} = 0.031 \pm 0.002$ nM/s^{-1}, $K_M = 20.5 \pm 3.0$ nM, $r_P = 3.21 \pm 0.04$ au nM^{-1}, and $p_0 = -1.03 \pm 0.54$ au, where the arbitrary unit (au) is the percentage of the product formed.

mechanism without product inhibition. These results indicate that product inhibition can be neglected in the progress curve analysis.

*Preincubation Experiments with Inhibitors **2** and **3**.* In these experiments we have investigated whether the 4-aza-steroid, **2**, saturated at C-1 and C-2, or the 6-aza-steroid **3** (Figure 1), were time-dependent inhibitors of the type I and II 5α-reductases. The concentration of testosterone was set to a value below the Michaelis constant ($K_M = 7$ μM for type I, 20.5 nM for type II) so that the reactions were approximately first-order in testosterone. No inhibitor except finasteride showed any time dependence with the type I enzyme (data not shown). The results for the type II enzyme are shown in Figure 3. Finasteride, **1**, and the 6-aza-steroid, **3**, but not the 4-aza-steroid **2**, are time-dependent inhibitors.

*Time-Dependent Inhibition by the 6-Aza-Steroids **3**–**6**.* Several 6-aza-steroids with structural modifications at either the C-4 or N-6 position were further investigated for time-dependent inhibition of the type II enzyme. The results from the preincubation experiments with the modified 6-aza-steroids are shown in Table 1. The apparent inhibition constants decreased 20-, 60-, and 80-fold over a 20 min period for **3**, **4**, and **5**, respectively. In contrast, the N-6 substituted derivative **6** showed very little inhibition and no observable time dependence.

Reversibility of Inhibition of 5α-Reductase II. Because finasteride is a slow binding inhibitor and was shown to irreversibly inhibit the reductases, the 6-aza-steroid **3** was tested to determine if it was a reversible inhibitor. After incubation, centrifugation of the microsomes, and resuspen-
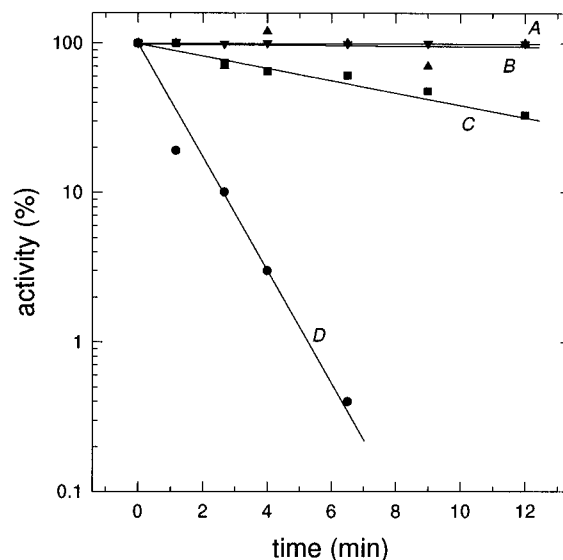

FIGURE 3: Simultaneous least-squares fit of substrate progress curves (5α-reductase II, pH 6.0, 37 °C) to eq 4 and the system of differential eqs 6a–d. The constant parameters were $[E]_0 = 0.01$ nM, and $p_0 = 0$. Substrate concentrations were 8, 16, 40 80, and 160 nM, respectively, for curves A–E. The best-fit values and standard errors of adjustable parameters were $k_2 = (1.48 \pm 0.57)$ s^{-1}, $k_3 = (0.644 \pm 0.024)$ s^{-1}, and $r_P = (647 \pm 29) \times 10^3$ cpm nM^{-1}. Loss of residual enzyme activity upon preincubation of type II 5α-reductase (4.0 nM) with finasteride **1** (10 nM, circles), compound **3** (10 nM, squares), and compound **4** (10 nM, triangles pointing up). Control (no inhibitor) is represented by triangles pointing down. See Experimental Procedures for details.

Table 1: Apparent Inhibition Constants with or without Preincubation of a Given Inhibitor (0–20 nM) with Type-II 5α-Reductase (0.1–0.2 nM)

	K_{app} (nM)[a]		
inhibitor	$t = 0$ min	$t = 10$ min	$t = 20$ min
finasteride	7.5 ± 2.5		0.2[b]
3	24 ± 2.1	0.97 ± 0.59	0.77 ± 0.51
4	130 ± 13	2.2 ± 1.3	1.8 ± 0.84
5	85 ± 15	1.7 ± 1.2	1.0 ± 0.75
6	4000	4000	4000

  [a] Enzyme was preincubated with varying concentrations of inhibitor for 0, 10, or 20 min before the assay. Remaining enzyme activity was measured in a 3 min assay. Assay conditions are described in Experimental Procedures. [b] After preincubation of enzyme and inhibitor for 20 min, residual enzyme activity was measured in a 40 min assay.

sion of the pellet in the absence of inhibitors, the enzyme activity was preserved. From the rate of product formation, the recovered enzyme concentration could be estimated as approximately 0.02 nM. Upon treatment with finasteride, the enzyme lost its activity completely and irreversibly. In contrast, upon treatment with compound **3**, the enzyme activity was partially recovered, and the reduction of testosterone was observed at a steady-state velocity of approximately 30% relative to the control (see Figure 4).

*Simplified Progress Curve Analysis for Finasteride and 6-Aza-Steroid **3**.* The reaction progress was analyzed by two different methods. The results of a preliminary analysis, based on the assumption of rapid equilibrium, are shown for compound **3** in Figures 5 and 7. The progress curves obtained at 8, 16, 32, and 68 nM inhibitor were fitted individually to eq 3. The best-fit values of adjustable parameters, for each concentration of the inhibitor, are listed
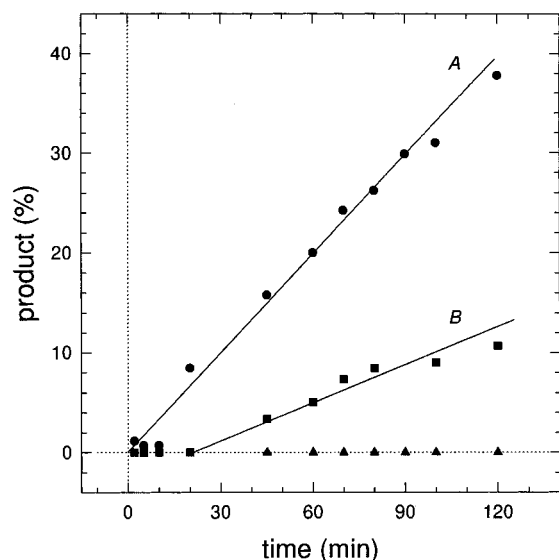
FIGURE 4: Recovery of activity after 5-AR was preincubated with finasteride (closed triangles), compound **3** (closed squares), or control (no inhibitor) represented by closed circles. See Experimental Procedures for details.

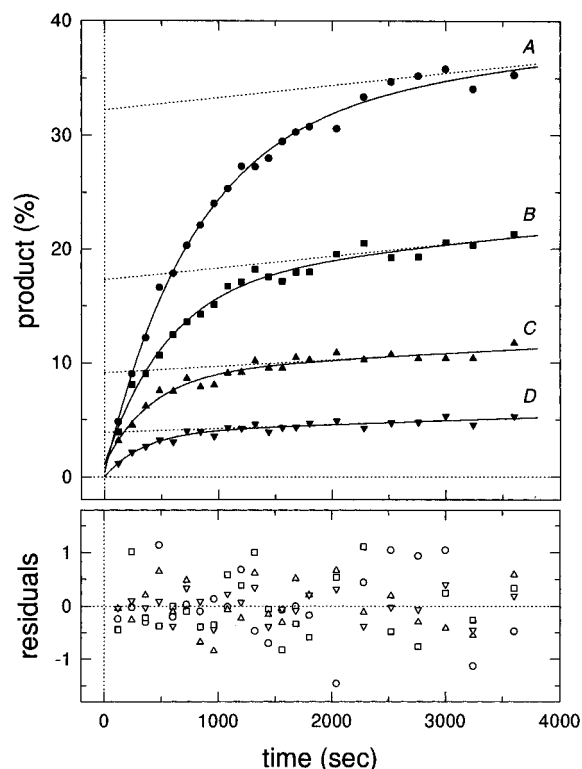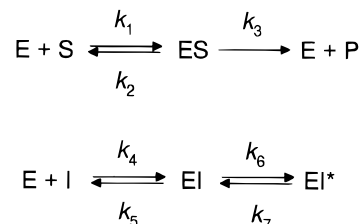FIGURE 5: Least-squares fit of progress curves from the inhibition of type II 5α-reductase (0.05 nM) by 6-aza-steroid **3** to eq 3. The initial substrate concentration was 31 nM. The inhibitor concentrations were 8, 16, 32, and 68 nM for curves A−D, respectively. For experimental condition and the best-fit values of adjustable parameters see text.

in Table 2. For a one-step inhibition mechanism, without an intermediate enzyme−inhibitor complex, the initial velocity v_0 should be constant, and the apparent rate constant k_{app} should increase linearly with the inhibition concentration $[I]_0$. These properties of the one-step mechanism are expressed in eqs 7a−c (Szedlacsek & Duggleby, 1995).

$$v_0 = V_{max}[S]_0/([S]_0 + K_M) \tag{7a}$$

$$v_s = V_{max}[S]_0/([S]_0 + K_M(1 + [I]_0/K_i)) \tag{7b}$$

$$k_{app} = k_7 + k_6[I]_0/(1 + [S]_0/K_M) \tag{7c}$$

On the other hand, for a two-step mechanism (Scheme 1), the initial velocity should decrease with the inhibitor concentration, by following a typical binding curve, and the apparent rate constant should depend on $[I]_0$ as a hyperbola, according to eqs 8a−c.

$$v_0 = V_{max}[S]_0/([S]_0 + K_M(1 + [I]_0/K_i)) \tag{8a}$$

$$v_s = V_{max}[S]_0/([S]_0 + K_M(1 + [I]_0/K_i^*)) \tag{8b}$$

$$k_{app} = k_7 + k_6([I]_0/K_i)/(1 + [S]_0/K_M + [I]_0/K_i) \tag{8c}$$

The parameters listed in Table 2 favor the two-step mechanism, because the initial velocity does decrease with the concentration of the inhibitor, as predicted by eq 8a. Also, the increase of the apparent rate constant with $[I]_0$ is hyperbolic, instead of linear. The nonlinear least-squares fit of v_0, v_s, and k_{app} to eqs 8a−c is shown in Figure 6. From fitting of v_0 to eq 8a, the dissociation constant K_i of the initial complex is 6.81 ± 0.24 nM; the fitted value of V_{max} is 0.099 ± 0.001 au s^{-1}, in good agreement with the substrate kinetic analysis (V_{max} was 0.098 au s^{-1} from fitting the substrate progress curve in Figure 2). From fitting of v_s to eq 8b, the overall dissociation constant K_i^* is 0.073 ± 0.015 nM; the fitted value of V_{max} is 0.098 ± 0.001 au s^{-1} in this case. From fitting of k_{app} to eq 8c, the initial inhibition constant K_i was 7.73 ± 0.52 nM. The isomerization rate constants were $k_6 = (3.52 ± 0.04) \times 10^{-3}$ s^{-1} and $k_7 = (0.25 ± 0.06)$

Table 2: Best-Fit Values of Adjustable Parameters, Obtained in Fitting the Progress Curves Shown in Figure 5 (0.05 nM Type II 5α-Reductase, 31 nM Testosterone, pH 6.0, 37 °C) to Equation 3

$[I]_0$ (nM)	$10^3 v_0$ (%P s^{-1})	$10^3 v_s$ (%P s^{-1})	$10^3 k_{app}$ (s^{-1})
0.0	59.1^a	59.1^a	
8.0	41.6 ± 3.9	1.07 ± 0.87	1.27 ± 0.17
16.0	30.6 ± 4.7	1.04 ± 0.44	1.82 ± 0.30
32.0	20.1 ± 5.3	0.55 ± 0.24	2.44 ± 0.55
68.0	11.8 ± 4.2	0.34 ± 0.12	2.97 ± 0.82

^{a} Initial velocity from fitting the substrate progress curve shown in Figure 1.

Scheme 1

$$E + S \underset{k_2}{\overset{k_1}{\rightleftarrows}} ES \overset{k_3}{\longrightarrow} E + P$$

$$E + I \underset{k_5}{\overset{k_4}{\rightleftarrows}} EI \underset{k_7}{\overset{k_6}{\rightleftarrows}} EI^*$$

$\times 10^{-3}$ s^{-1}, from which the total dissociation constant K_i^* $= K_i k_7/k_6$ is 0.55 nM.

Similar analysis, by using the two-step model equation, was performed for finasteride progress curves (data not shown). In this case the steady-state velocity v_s in eq 3 was set to zero by default, because finasteride is an irreversible inhibitor. For the same reason, k_7 in eq 8c was set to zero as well. Nonlinear regression of the apparent rate constant k_{app} vs inhibitor concentration yielded K_i = 11.9 ± 4.1 nM and k_6 = 0.09 ± 0.01 s^{-1} as the best fit values.
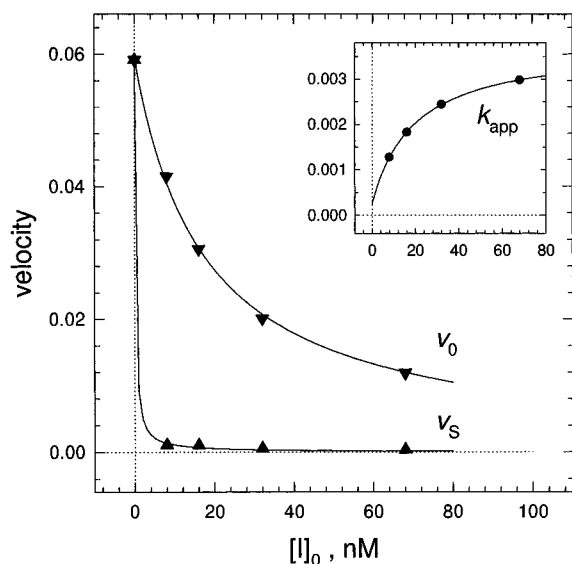
FIGURE 6: Least-squares fit of the initial velocities v_0 from Table 2 to eq 8a, the steady-state velocity v_s to eq 8b, and the apparent first-order rate constant k_{app} to eq 8c. The best fit values of adjustable parameters K_i, K_i^*, k_6, and k_7 are listed in the text.
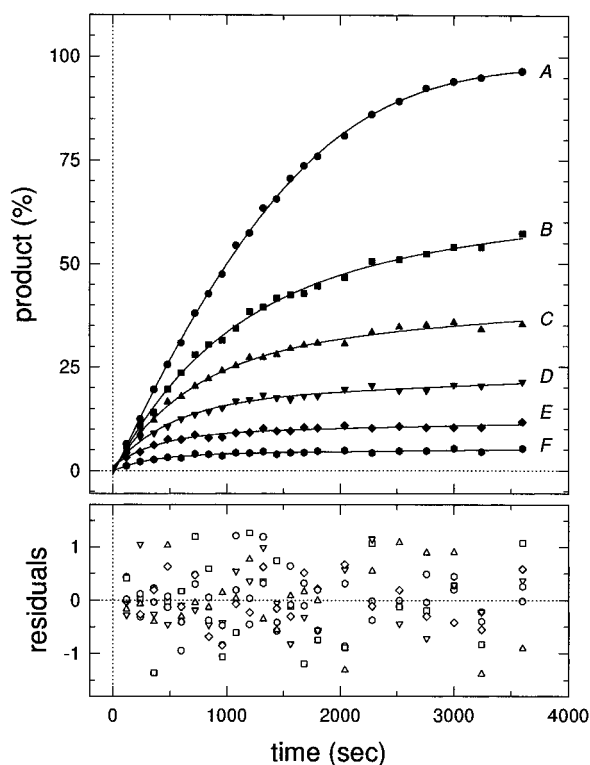

FIGURE 7: Least-squares fit of progress curves from 5α-steroid reductase II inhibition by 6-aza-steroid **3**. The inhibitor concentrations were 0, 4, 8, 16, 32, and 68 nM for curves A−F, respectively. The substrate concentration (31 nM) was assumed constant for all datasets. The enzyme concentration was assumed constant (0.05 nM) for curve A or variable within 10% titration error (curves B−F). The best fit values of optimized parameters are listed in the text.

The inhibition progress curves for compound **3** were analyzed more thoroughly, by using a complete differential model where the rapid equilibrium assumption is not made. The collection of progress curves in Figure 7 were fitted as a whole to the system of eqs 4 and 5. The constant parameters were the initial concentration of the substrate ($[S]_0$ = 31 nM) and the inhibitor ($[I]_0$ = 0, 4, 8, 32, 68 nM), the initial concentration of the enzyme in the assay where

inhibitor was absent ($[E]_0$ = 0.05 nM), and the bimolecular rate constant for the formation of the Michaelis complex (k_1 = 100 μM^{-1} s^{-1}). The best fit values of globally optimized parameters were k_2 = 1.44 ± 0.10 s^{-1}, k_3 = 0.61 ± 0.02 s^{-1}, k_4 = 5.1 μM^{-1} s^{-1}, k_5 = (32.6 ± 8.0) × 10^3 s^{-1}, k_6 = (3.49 ± 0.72) × 10^3 s^{-1}, k_7 = (0.076 ± 0.019) × 10^3 s^{-1}, and r_P = 3.20 ± 0.01. All enzyme concentrations in assays where the inhibitor was present were considered as locally optimized parameters, within the estimated ±10% titration error. The best fit values of locally optimized concentrations were $[E]_0$ = 0.053 ± 0.003 nM, $[E]_0$ = 0.052 ± 0.003 nM, $[E]_0$ = 0.052 ± 0.003 nM, $[E]_0$ = 0.048 ± 0.007 nM, and $[E]_0$ = 0.048 ± 0.007 nM, for the assays at 4, 8, 16, 32, and 64 nM inhibitor, respectively. From the best-fit values of rate constants k_4 and k_5, the dissociation constant of the initial complex, K_i, was calculated as k_5/k_4 = 6.5 nM. Similarly, the overall dissociation constant of the final complex, K_i^*, was calculated as $k_5 k_7/k_4 k_6$ = 0.14 nM. This value is bracketed by the results obtained by the simplified method above, as shown in Table 3 (K_i^* = 0.07 nM and 0.55 nM by using eq 8b or 8c, respectively). The traditional method of apparent first-order rate constants is based on several simplifying assumptions discussed below. Therefore, the value of K_i^* given by the general method of analysis is more reliable. The merits of both methods are compared in the Discussion.

The uncertainties of rate constants, given above, are projections into the subspace of k_4, because this parameter was so strongly correlated with k_5, k_6, and k_7 that the asymptotic standard errors (based on the linear regression model) became meaningless. Therefore the 68% confidence interval of k_4 was determined by complete search of the chi-square hypersurface. In this procedure, the value of k_4 was held constant at progressively larger or smaller values around the best-fit estimate, and all remaining parameters were optimized by nonlinear regression at each step. The results are summarized in Figure 8. The absolute minimum on the chi-square hypersurface was found at k_4 = 5.1 μM^{-1} s^{-1}, and the 68% confidence interval consisted of values between 3 and 120 μM^{-1} s^{-1}. Larger values of k_4 than the upper bound of this interval were not investigated, because the solution of the differential eqs 5 became unstable. Within this interval, the remaining rate constants attained their best-fit values in the range 0.030−0.860 s^{-1} for k_5, 0.0034−0.007 s^{-1} for k_6, and 0.00007−0.00011 s^{-1} for k_7. At each step along search path, the dissociation constants K_i and K_i^* were computed from the best-fit values of rate constants. The shaded area in Figure 8 enclose the 68% probability interval. Thus there is 68% probability that the initial K_i is between 6 and 10 nM, and that the final K_i^* is between 0.14 and 0.2 nM. The kinetic constants determined in this study are summarized in Table 3.

DISCUSSION

Previous reports demonstrated that Δ^1-4-aza-steroids such as finasteride were irreversible inhibitors of the 5α-reductases (Tian et al., 1994; Faller et al., 1993). In this study we further investigated the mechanism of inhibition of type II 5α-reductase by finasteride and compared the results with other aza-steroid inhibitors.

Results from the progress curve experiments demonstrate that both finasteride and the 6-aza-steroid **3** inhibit the type

Table 3: Summary of Kinetic Constants for Finasteride and the 6-Aza-Steroid **3**[a]

inhibitor	method	K_i (nM)	K_i^* (nM)	k_4 ($\mu M^{-1}\ s^{-1}$)	$10^3\ k_5$ (s^{-1})	$10^3\ k_6$ (s^{-1})	$10^3\ k_7$ (s^{-1})
finasteride	B[c]	11.9 ± 4.1	0.0[f]			0.09 ± 0.01	0.00[f]
3	A[b]	6.81 ± 0.24	0.073 ± 0.015				
3	B	7.73 ± 0.52	0.55			3.52 ± 0.04	0.25 ± 0.06
3	C[d]	6.5 ± 2.1[g,h]	0.14 ± 0.05[g,h]	5	32.6 ± 8.0	3.49 ± 0.72	0.076 ± 0.019
3	D[e]	6.5[g] (6.0–10)	0.14[g] (0.14–0.20)	5 (3–120)[i]	32 (30–860)	3.5 (3.4–7)	0.08 (0.07–0.11)

[a] Uncertainties of parameters expressed with the "±" sign are standard errors from nonlinear regression. Values in parentheses are 68% confidence intervals obtained by systematic search in the parameter space. [b] From fitting initial velocities v_0 and pseudo-steady-state velocities v_s to eqs 8a and 8b, respectively. [c] From fitting apparent first-order rate constants to eq 8c. [d] From fitting progress curves to differential eqs 5a–c; confidence intervals are standard errors from least-squares fit. [e] As in method C; confidence intervals determined by a search in parameter space. [f] Assumed irreversible inhibition. [g] Computed from rate constants. [h] Uncertainties from error propagation theory (Bevington, 1969), taking into account covariances of rate constants. [i] Confidence interval search terminated at the upper level indicated (120 $\mu M^{-1}\ s^{-1}$).
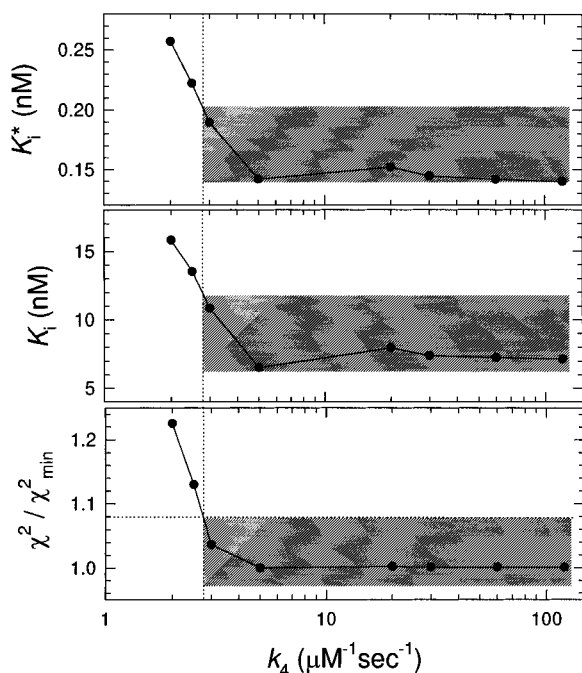

FIGURE 8: Confidence interval determination for bimolecular association rate constant k_4 and equilibrium constants K_i and K_i^*. Rate constant k_4 was held constant at various values, lower or higher than the best fit value, and all the remaining parameters in the kinetic model (Scheme 1) were optimized. At each step, the equilibrium constants were computed from the best-fit values of rate constants. The shaded areas enclose the 68% probability interval, as determined by the F-statistic.

II enzyme via at least a two-step mechanism. The dissociation constants for the initial rapid equilibrium complexes are comparable for both inhibitors, which indicates that the enzyme does not prefer the Δ^1-4-aza steroid ring structure over the 6-aza-steroid structure. However, dramatic differences between the two inhibitors were observed in terms of reversibility experiments. Finasteride irreversibly inhibits the type II enzyme [see also Faller et al. (1993)], whereas **3** is a reversible inhibitor. Interestingly, the rates of forming the final enzyme–inhibitor complex are different for the 4- and 6-aza-steroids. The k_6 is approximately an order of magnitude larger for finasteride than for **3**. Direct comparisons are difficult because inhibition by finasteride encompasses a chemical transformation step at the 1,2 double bond (Tian et al., 1995). In preliminary experiments we did not find any evidence for chemical transformations of 6-aza-steroids upon incubation with the enzyme. Regardless of the nature of slow binding step, finasteride can be classified as a more potent inhibitor of the type II enzyme, because it is irreversible.

A cautionary note is due with regard to the proposed kinetic mechanisms of the transient inhibition by compound **3** (Scheme 1). The kinetic data by no means prove that this EI $\rightleftarrows$ EI* inhibition mechanism is in fact operating. The data only exclude the single-step kinetic mechanism, because the initial velocities v_0 obtained by fitting progress curves to eq 3 do depend on the concentration of the inhibitor, as is predicted by the two-step model, but not by the one-step model.

Equations 3, 7, and 8, which were used to discriminate between the kinetic models, are based on four simplifying assumptions: (i) that the rate of association and dissociation of the enzyme–inhibitor complex is infinitely faster than any other step in the inhibition mechanism; (ii) that the inhibitor is so weak that the fraction of enzyme-bound inhibitor can be neglected; (iii) that the final change in substrate concentration is so small, or the ratio $[S]_0/K_M$ is so large, that velocity change due to substrate depletion can be neglected; and (iv) that the substrate is present in an infinite excess over the enzyme. In fact only the last assumption is perfectly valid. The rapid equilibrium approximation seems justified, because a fit of the complete differential model suggests that the dissociation rate constant k_5 is about 10 times higher than the isomerization rate constant k_6. The assumption of weak binding can be defended also, because the enzyme concentrations used (0.05 nM) were much smaller than the inhibitor concentrations (8–68 nM). Otherwise the classical treatment would break down, because the overall inhibition constants (0.14 nM) is indeed comparable with the enzyme concentration ("tight binding"). The relative decrease in velocity due to substrate depletion at 30% conversion is $1 - (1 + K_M/[S]_0)/(1 + K_M/0.7[S]_0) = 0.15$ or 15%. Thus the assumption of constant velocity holds fairly enough.

A very serious problem for the classical, rapid equilibrium method of transient inhibition analysis (eqs 3, 7, and 8) is that one cannot obtain reliable estimates of the steady state velocity v_s, and of the first-order rate constant k_{app}, from progress curves collected at relatively low inhibitor concentrations (e.g., 8 nM, curve A in Figure 6). This is the reason why the traditional method gave quite different estimates of the overall inhibition constant K_i^*, namely, 0.07 nM from v_s (eq 8b) and 0.55 nM from k_{cat} (eq 8c). Even though the experimental error is low (standard error of the HPLC determination is less than 1% in this case), the classic method requires that, even with the data of this quality, the total reaction time should be approximately 10 times longer than the half-time of the transient phase (approximately 4500 s for the curve at 8 nM inhibitor). Unfortunately, this

requirement cannot be satisfied without significantly lowering the enzyme concentration, because already at time 3600 s, about 40% of the the substrate was consumed. Thus, extending the reaction time beyond this point would not lead to true steady state in any case, because of the progressive substrate depletion. Lowering the enzyme concentration for only some progress curves in the global dataset is not a practical solution.

In contrast, the modern numerical method does not impose any artificial requirements on the experiment, for the sole purpose of obtaining approximately linear progress curves ("steady state"). For example, when using the general numerical method based on differential equations, even the progress curve collected at 4 nM inhibitor (curve B in Figure 7), where the substrate depletion reaches 60%, is a valid and informative dataset.

The rapid equilibrium method, which is the standard approach in early literature on time-dependent inhibition, is incapable of handling alternative mechanisms of transient inhibition, such as $E^* \rightleftarrows E + I \rightleftarrows EI$ and $I^* \rightleftarrows I + E \rightleftarrows EI$. In this paper we used this method mostly for comparison with the more recent alternative, namely, a fully general approach based on numerical integration of differential equations. This approach makes no assumptions about the relative magnitude of rate constants, or about the inhibitory potency, or about the concentration ratios used in the experiment. This general method not only provided us with estimates of the association and dissociation rate constants, but it was also more successful in pinpointing the values of rate constants for isomerization. When the general numerical method was applied to the mechanisms $E \rightleftarrows E^*$ and $I \rightleftarrows I^*$, these mechanisms were excluded because they showed exactly the same mismatch between the data and model, as did the simplest mechanism of all, $E + I \rightleftarrows EI$. Altogether six candidate mechanism were tested but only one, $E + I \rightleftarrows EI \rightleftarrows EI^*$, was found acceptable. The details of this model discrimination analysis will be presented elsewhere.

The main goal of this study was to understand which structural features in *de novo* inhibitors of the 5α-reductase are responsible for relatively slow onset of inhibition. The comparison of apparent inhibition constants in Table 1 shows that the structural requirements for slow binding inhibition of the type II isozyme are diverse. Certain structural modifications of the 6-aza-steroids do not impair their ability to act as time-dependent inhibitors. Slow binding is still observed when 6-aza-steroids are altered through methyl substitutions at C-4 or N-6. Also, preliminary investigations showed that modifications at C-17 do not abolish slow onset of inhibition. However, the placement of an acetyl function on N-6 was a substitution that prevented the 6-aza-steroid from acting as a slow binding inhibitor. It is not clear if the slow binding was perturbed because of electronic effects via localization of the nitrogen electrons into the carbonyl oxygen, since the inhibition constant was altered 1000-fold compared to the other 6-aza-steroids. Characterization of additional 6-aza-steroids that have N-6 substitutions could aid in determining which structural features are responsible for relatively slow onset of inhibition.

REFERENCES

Anderson S., & Russell, D. W. (1990) *Proc. Natl. Acad. Sci. U.S.A.* *87*, 3640−3644.

Anderson, S., Berman, D. M., Jenkins, E. P., & Russell, D. W. (1991) *Nature 354*, 159−161.

Bevington, P. R. (1969) *Data Reduction and Error Analysis for the Physical Sciences*, p 60, McGraw-Hill, New York.

Duggleby, R. G. (1986) *Biochem. J. 235*, 613−616.

Faller, B., Farley, D., & Nick, H. (1993) *Biochemistry 32*, 5705−5710.

Frye, S. V., Haffner, C. D., Maloney, P. R., Mook, R. A., Hiner, R. N., Batchelor, K. W., Bramson, H. N., Stuart, J. D., Schweiker, S. L., Vanarnold, J., Bickett, D. M., Moss, M. L., Tian, G. C., Unwalla, R. J., Lee, F. W., Tippin, T. K., James, M. K., Grizzle, M. K., Long, J. E., Schuster, S. V., & Dorsey, G. F. (1993) *J. Med. Chem. 36*, 4313−4315.

Frye, S. V., Haffner, C. D., Maloney, P. R., Mook, Jr., R. A., Dorsey, G. F., Jr., Hiner, R. A., Batchelor, K. W., Bramson, H. N., Stuart, J. D., Schweiker, S. L., van Arnold, J., Bicket, D. M., Moss, M. L., Tian, G. C., Umwalla, R. J., Lee, F. W., Grizzle, M. K., Long, J. E., & Schuster, S. V. (1994) *J. Med. Chem. 37*, 4313−4315.

Hindmarsh, A. C (1983) in *Scientific Computing* (Stepleman, R. S., Ed.) pp 55−64, North Holland, Amsterdam.

Jenkins, E. P., Anderson, S., Imperato-McGinley, J., Wilson, J. D., & Russell D. W. (1992) *J. Clin. Invest. 89*, 293−300.

Liang, T., Cascieri, M. A., Cheung, A. H., Reynolds, G. F., & Rasmusson, G. H. (1985) *Endocrinology 117*, 571−579.

Morrison, J. F. (1982) *Trends Biochem. Sci. 7*, 102−105.

Morrison, J. F., & Walsh, C. T. (1988) *Adv. Enzymol. Relat. Areas Mol. Biol. 61*, 201−301.

Rasmusson, G. H., Berman, C., Brooks, J. R., Cascieri, M. A., Cheung, A. H., Liang, T. M., Patel, G. F., Reynolds, G. F., Steinberg, N. G., & Walton, E. (1986) *J. Med. Chem. 29*, 2298−2315.

Reich, J. G. (1992) *Curve Fitting and Modelling for Scientists and Engineers*, McGraw-Hill, New York.

Smith, R. A., Wake, R., & Soloway, M. S. (1988) *Postgrad. Med. 83*, 79−81.

Szedlacsek, S. E., & Duggleby, R. G. (1995) *Methods Enzymol. 249*, 144−180.

Thigpen, A. E., Silver, R. I., Guileyardo, J. M., Casey, M. L., McConnell, J. D., & Russell, D. W. (1993) *J. Clin. Invest. 92*, 903−910.

Tian, G., Stuart, D., Moss, M, Domanico, P., Bramson, N., Patel, I. R., Kadwell, S., Overton, L. K., Kost, T. A., Mook, R., & Wiseman, J. (1994) *Biochemistry 33*, 2291−2296.

Tian, G., Chen, S.-Y., Facchine, K. L., & Prakash, S. (1995) *J. Am. Chem. Soc. 117*, 2369−2370.

Vialard, J., Lalumiere, M., Vernet, T., Briedis, D., Alkhatib, G., Henning, D., Levin, D., & Richardson, C. (1990) *J. Virol. 64*, 37−50.

Wilson, J. D. (1980) *Am. J. Med. 68*, 745−756.

BI952472+